Available online at www.sciencedirect.com
ScienceDirect
Geochimica et Cosmochimica Acta 71 (2007) 5405–5422
Geochimica et Cosmochimica Acta
www.elsevier.com/locate/gca

Alteration effects of volcanic ash in seawater: Anomalous Y/Ho ratios in coastal waters of the Central Mediterranean sea

P. Censi [a,e,*], M. Sprovieri [b], D. Larocca [c], P. Aricò [c], F. Saiano [d], S. Mazzola [e], P. Ferla [c]

[a] *Dipartimento di Scienze Geologiche, Università di Catania, Corso Italia, 55, 95129 Catania, Italy*
[b] *I.A.M.C.-CNR, Calata Porta di Massa (Interno Porto di Napoli), 80133 Napoli, Italy*
[c] *Dipartimento C.F.T.A., Università di Palermo, via Archirafi 36, 90123 Palermo, Italy*
[d] *Dipartimento I.T.A.F., Università di Palermo, Viale delle Scienze 13, 90128 Palermo, Italy*
[e] *I.A.M.C.-CNR, via L. Vaccara 61, 91026 Mazara del Vallo (Tp), Italy*

Received 31 August 2006; accepted in revised form 6 September 2007; available online 26 October 2007

Abstract

This paper presents the results of a study based on data collected during the oceanographic cruise ANSIC 2001 carried out in the Ionian Sea during the explosive activity of Mount Etna in the summer of 2001. Anomalous low values of Y/Ho ratios in seawater suggest extensive scavenging processes on the surfaces of smectitic alteration products, with Y and Ho fractionation controlled by the differences in their electronic configurations and behaviour during solution/surface complexation equilibria. These processes can also be traced through the presence of significant tetrad effects recorded in the chondrite-normalised Rare Earth Elements and Yttrium (YREEs) patterns of suspended particulate matter. This suggests that the preferential Y scavenging from seawater is due to the formation of inner-sphere complexes with OH^- groups on montmorillonite crystal surfaces. The preliminary results of kinetic experiments of YREE released from volcanic ash to coexisting seawater, and the related effects on Y/Ho ratios and Ce anomalies, are consistent with the fractionation of Light Rare Earth Elements (LREEs) with respect to Heavy Rare Earth Elements (HREEs) observed in dissolved phase. They suggest a behaviour of Y similar to that reported for LREEs, particularly for Ce and Pr.

1. INTRODUCTION

Intense research activity during the last 25 years has focused on a more accurate understanding of the chemical and physical processes that regulate the distribution of Rare Earth Elements and Yttrium in seawater (Goldberg et al., 1963; Cantrell and Byrne, 1987; Elderfield, 1988; Goldstein and Jacobsen, 1988; Greaves et al., 1991). This research has aimed to: (i) evaluate their status of complexation (Cantrell and Byrne, 1987; Koeppenkastrop et al., 1991; Koeppenkastrop and De Carlo, 1992; Lee and Byrne, 1992; Millero, 1992); (ii) recognise YREE fractionation processes between dissolved and suspended phases (Elderfield et al., 1990; Alibo and Nozaki, 1999; Tachikawa et al., 1999; Quinn et al., 2004); (iii) examine the capability of YREEs as tracers of anthropogenic inputs both in rivers and coastal waters, especially in areas characterised by high population densities (e.g., Bau and Dulski, 1996); and (iv) evaluate the input mechanisms of these elements in seawater from atmospheric and riverine loads (Sholkovitz, 1993; Sholkovitz et al., 1999; Hannigan and Sholkovitz, 2001; Aubert et al., 2002).

Studies concerning the release of YREEs during rock-water interaction are scarce (Bau et al., 1998; Sholkovitz et al., 1999: Takahashi et al., 2002; Bau et al., 2004), and there is little data on the processes that regulate the alteration of volcanic materials at low temperature and in seawater (e.g. Pichler et al., 1999).

* Corresponding author.
E-mail address: censi@irma.pa.cnr.it (P. Censi).

0016-7037/$ - see front matter © 2007 Elsevier Ltd. All rights reserved.
doi:10.1016/j.gca.2007.09.015

In particular, the fate of YREEs during the latter processes is influenced by:

- Their behaviour in the dissolved phase, strongly driven by hydrolysis and complexation equilibria (Byrne and Li, 1995; Byrne and Liu, 1998; Klungness and Byrne, 2000; Luo and Byrne, 2004; Sonke and Salters, 2006; Pourret et al., 2007);
- Their sorption (surface complexation) on particles and colloids (Davranche et al., 2004, 2005);
- Their scavenging effects on the alteration surfaces of newly formed mineral phases.

These mineral phases are essentially represented by poorly-crystallised montmorillonite-like phases that show both permanent negative charges in surface layers, due to isomorphic substitutions, and pH-dependent charges located on the hydroxyls, at the edges (Tombácz and Szekeres, 2004). The behaviour of the dissolved YREEs in the presence of montmorillonite was investigated by Takahashi et al. (2004), and Coppin et al. (2002), although the latter authors excluded Yttrium from their investigation.

The intense volcanic activity of Mount Etna during 2001 provided a unique opportunity to simultaneously monitor YREE distribution in unaltered atmospheric particulate matter, seawater, and suspended particulate matter (SPM). The eruption took place on the upper slopes of Mount Etna between July 13 and August 9.

This study combines extensive data sampling, precise YREE compositional data, and the results of reaction kinetic experiments to fill the knowledge gap regarding Lanthanide release to seawater during volcanic activity. Furthermore, we recognise that the "anomalous" Y/Ho ratios in seawater observed in this study represent a geochemical proxy indicative of the adsorption processes occurring in the marine environment.

2. SAMPLING STRATEGIES AND ANALYTICAL METHODS

2.1. Sampling

Samples were collected during the ANSIC 2001 cruise at six sampling stations along the Ionian coast of Sicily

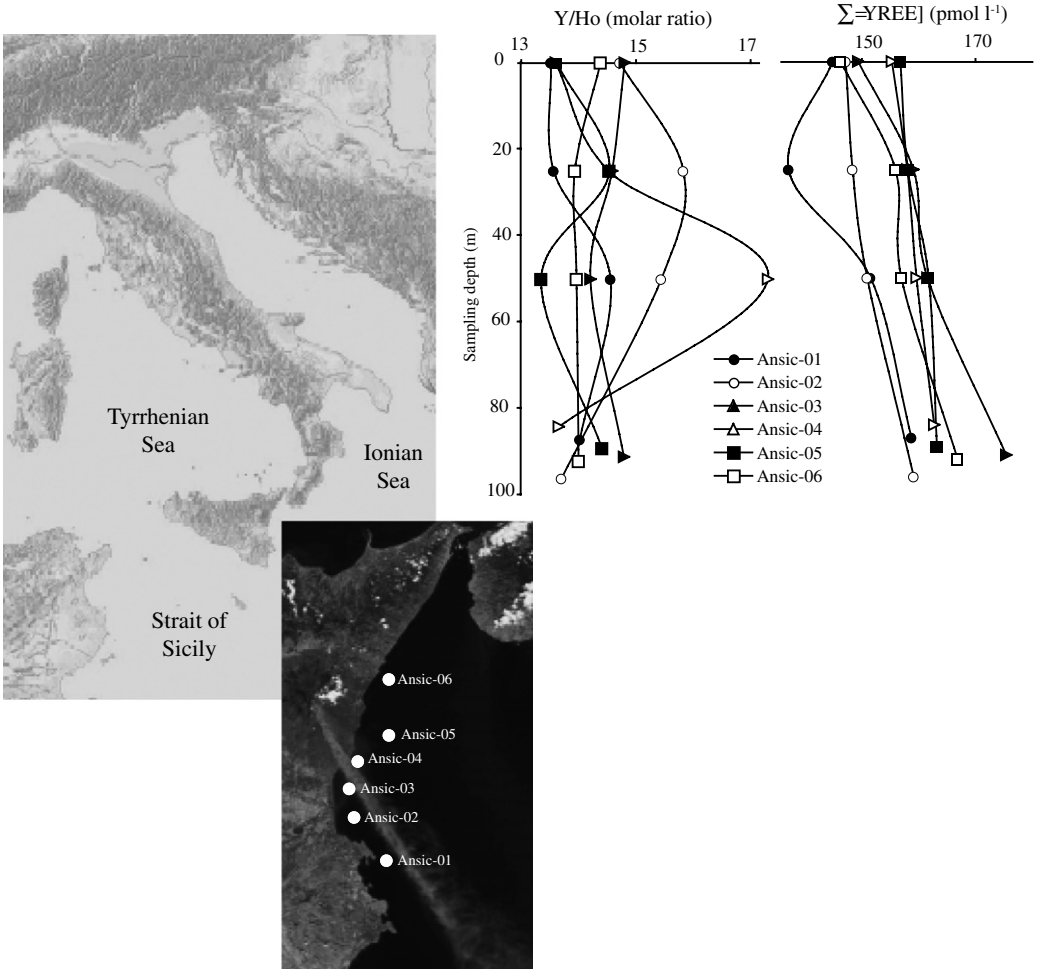

Fig. 1. Location of sampling sites. Satellite image showing the Etna plume during volcanic activity in 2001 is provided by www.visibleearth.nasa.gov/view_detail.php?id=1868. YREE concentrations and Y/Ho profiles are reported for the six studied sampling stations.

in the early summer of 2001, aboard the RV "Urania" (Fig. 1).

The sampling system consisted of a Neil-Brown CTD rosette frame and 24 × 12 l teflon-lined GoFlo bottles. Upon recovery of the GoFlo bottles, water samples were immediately filtered through 0.2 μm Millipore® filters using a teflon filtering manifold in order to reduce further dissolution of the labile particulate fraction (FengFu et al., 1997); they were then acidified to pH 1–2 with HNO_3 Merck, ULTRAPURE®. All the water samples were processed in a laminar flow clean bench to minimise contamination, and all sampling materials were previously cleaned with high purity grade reagents (Merck, ULTRAPURE®). All the materials used to collect and manipulate water samples were plasticware and were acid cleaned with 1:10 hot high purity HNO_3 solutions.

Volcanic ash was collected during the activity of Mount Etna with a polyethylene plate with a surface area of 1 m^2 that was located on the roof of the Department of Geology of the University of Catania for 5 days in July 2001 (no rainfall occurred in this period). At the end of the collection period, the thickness of volcanic ash was measured to be about 2.15 cm.

2.2. Seawater analysis

In order to increase the accuracy of the seawater YREE analysis, each sample (2000 ml) was pre-concentrated with CHELEX 100® (200–400 mesh) chelating resin. The pH value, measured according to Butler et al. (1985), Dickson (1993a,b), and Millero et al. (1993), of each seawater sample was adjusted to 6.0 with CH_3COONH_4, as described by Möller et al. (1992). The sample was loaded into an 8-cm long column filled with CHELEX-100, which had been previously cleaned and conditioned according to Paulson (1986). YREEs were eluted with 5 ml of HNO_3 3.5 M, yielding a 400-fold enrichment factor. Details of the procedures are reported in Paulson (1986) and Möller et al. (1992). Briefly, pH values in studied seawater samples were measured by a potentiometric method based on sequential measurements of the electromagnetic force of a cell, both in a buffer solution of defined pH and in the seawater sample, and referred to the total pH scale. In order to reduce the effects of the residual liquid-junction potential, standard buffer solutions were prepared using CH_3COONH_4 buffered synthetic seawater (35‰ salinity), according to Demianov et al. (1995).

In order to remove their YREE contents, 10 l of a seawater batch solution, hereafter referred to as SEA-1, were divided in five 2-l aliquots, each of which were filtered through a 0.2-μm filter, pH adjusted to 6.0, and loaded into an 8-cm long column filled with CHELEX-100, as previously described. Trace element scavenging on an ion exchange resin was repeated five times to ensure their complete removal. The efficiency of this approach was demonstrated by Möller et al. (1992) and Censi et al. (2004, 2005), and by the results obtained in this work (Table 1). A 500-μl aliquot of a standard solution of known YREE concentration was added to 5 l of the trace metals free seawater to yield an artificial seawater solution, hereafter referred to as SOL-1 (Table 1). The obtained solution was subdivided in five different aliquots labelled EL-1, EL-2, EL-3, EL-4, and EL-5, respectively. These were used to measure the recovery of each YREE, estimated based on the analysis of the five replicate samples. The results of estimated recovery for each YREE are reported in Table 1 and range from 88% for Er to 96% for Ce. The anal-

Table 1
Recoveries for each YREE calculated, after CHELEX-100 exchange resin treatment, for five different aliquots (EL-1–EL-5) of spiked, trace-element-free, seawater

	EL-1 (%)	EL-2 (%)	EL-3 (%)	EL-4 (%)	EL-5 (%)	Yield (%)	$\sigma\pm$ (%)	SEA-1 (pmol l^{-1})	1st run (pmol l^{-1})	2nd run (pmol l^{-1})	SOL-1 (pmol l^{-1})	Er_T (pmol l^{-1})
Y	90.5	94.0	93.0	93.9	91.2	92.5	1.6	117.76	8.81	0.66	11.25	0.03
La	95.1	92.4	96.1	92.3	92.9	93.8	1.7	82.84	5.17	0.32	7.20	0.04
Ce	97.3	93.8	101.1	92.2	96.6	96.2	3.4	100.18	3.81	0.15	7.14	0.03
Pr	90.7	92.3	88.0	90.5	90.4	90.4	1.5	12.91	1.24	0.12	7.10	0.04
Nd	92.3	94.9	91.5	95.7	96.4	94.2	2.1	55.73	3.25	0.19	6.93	0.02
Sm	96.8	98.4	97.6	92.3	92.9	95.6	2.8	10.89	0.48	0.02	6.65	0.02
Eu	90.2	93.4	92.8	87.6	91.1	91.0	2.3	2.33	0.21	0.02	6.58	0.02
Gd	91.8	89.2	90.1	87.0	91.5	89.9	1.9	10.16	1.02	0.10	6.36	0.03
Tb	93.1	96.4	93.9	91.2	96.7	94.3	2.3	1.75	0.10	0.01	6.29	0.04
Dy	93.9	96.6	88.9	94.3	96.8	94.1	3.2	10.22	0.60	0.04	6.15	0.04
Ho	93.5	89.6	95.4	88.6	89.5	91.3	3.0	2.28	0.20	0.02	6.06	0.03
Er	91.4	86.9	90.6	90.8	82.2	88.4	3.9	6.54	0.76	0.09	5.98	0.03
Tm	92.3	95.2	94.5	90.2	96.4	93.7	2.5	0.93	0.06	0.00	5.92	0.04
Yb	93.2	98.5	98.7	95.1	91.4	95.4	3.2	6.23	0.29	0.01	5.78	0.04
Lu	94.5	93.9	89.9	89.3	95.4	92.6	2.8	0.96	0.07	0.01	5.72	0.04

Mean and standard deviation values are also reported. YREE concentrations in the SEA-1 solution before of trace element removal after the first and the second stripping runs. See text for details. Measurement uncertainties for the investigated trace elements (Er_T) were estimated as total of: (i) the associated critical values (L_C), (ii) the detection limits (L_D), (iii) the limit of quantification (L_Q), and (iv) the estimated error for the CHELEX resin enrichment procedure, according to the "Water Research Centre Procedure for the Determination of L_C, L_D (and ISO/IUPAC determination of L_Q)" (see Water Research Centre procedure in www.epa.gov/waterscience/methods/det/faca/techworkgroup/index.html#detunder).

Table 2
Geographical location, sampling depth, temperature, salinity and YREE concentrations for the analysed seawater samples

	Long. (W)	Lat. (N)	Depth (m)	Temp. (°C)	Sal. (‰)	YREE concentrations (pmol l^{-1})															Y/Ho	Ce/Ce*	Eu/Eu*	t_3
						Y	La	Ce	Pr	Nd	Sm	Eu	Gd	Tb	Dy	Ho	Er	Tm	Yb	Lu				
Ansic-01	15.2870	37.3050	0	23.5	38.5	34.32	22.88	17.16	4.37	21.87	5.02	1.40	7.48	1.28	9.20	2.54	7.81	1.09	7.34	1.03	13.51	0.39	0.69	0.87
			25	18.9	38.3	32.63	21.84	16.24	4.20	20.71	4.22	1.20	7.60	1.22	8.72	2.41	7.26	1.00	6.84	0.98	13.56	0.39	0.63	0.84
			50	16.6	38.4	36.17	23.99	18.47	4.75	22.49	4.68	1.51	8.05	1.35	9.53	2.49	8.10	1.12	7.68	1.07	14.55	0.40	0.74	0.88
			87	15.7	38.5	37.81	25.36	19.32	4.60	23.95	4.97	1.65	8.15	1.42	9.98	2.70	8.59	1.19	7.89	1.07	14.01	0.41	0.78	0.89
Ansic-02	15.1931	37.4083	0	23.9	38.6	35.15	23.36	17.31	4.49	21.72	4.80	1.35	8.46	1.31	9.40	2.39	7.88	1.10	7.36	1.03	14.71	0.39	0.63	0.86
			25	19.2	38.4	35.29	23.57	17.53	4.42	22.25	4.77	1.38	8.33	1.32	9.47	2.23	8.03	1.11	7.54	1.04	15.82	0.39	0.65	0.91
			50	18.0	38.3	35.65	24.02	19.02	4.59	22.90	4.52	1.41	7.73	1.34	9.52	2.31	8.09	1.12	7.56	1.07	15.43	0.42	0.71	0.93
			96	16.4	38.4	38.03	25.36	18.40	4.94	24.11	5.39	1.55	8.15	1.39	10.21	2.78	8.50	1.13	7.99	1.13	13.69	0.38	0.71	0.87
Ansic-03	15.1773	37.4720	0	23.8	38.6	35.25	23.57	18.85	4.90	22.35	4.36	1.47	7.70	1.30	9.38	2.38	8.28	1.10	7.32	1.05	14.79	0.41	0.75	0.90
			25	19.2	38.3	37.92	25.52	18.89	4.80	23.84	5.16	1.61	7.96	1.43	10.25	2.60	8.67	1.20	8.00	1.14	14.58	0.39	0.76	0.93
			50	18.0	38.3	38.57	25.72	18.89	5.02	24.71	5.17	1.59	8.19	1.44	10.34	2.72	8.77	1.13	8.07	1.14	14.20	0.38	0.73	0.90
			91	16.4	38.4	41.86	27.96	20.81	5.48	26.41	5.49	1.66	9.19	1.57	11.24	2.83	9.42	1.31	8.84	1.24	14.78	0.39	0.70	0.91
Ansic-04	15.2031	37.5420	0	23.0	38.5	36.67	24.62	17.90	4.95	23.21	4.72	1.49	9.35	1.38	9.84	2.70	8.38	1.13	7.76	1.09	13.59	0.38	0.66	0.81
			25	19.6	38.3	37.58	24.97	19.75	4.75	23.81	4.69	1.53	8.12	1.40	10.00	2.59	8.50	1.18	7.90	1.11	14.52	0.42	0.74	0.90
			50	18.0	38.3	38.90	25.59	17.99	4.80	24.26	5.00	1.56	8.39	1.44	10.28	2.25	8.60	1.20	8.12	1.15	17.29	0.37	0.72	0.98
			84	16.1	38.5	38.72	25.92	19.27	4.86	24.30	5.29	1.63	8.56	1.44	10.41	2.84	8.98	1.20	8.04	1.15	13.64	0.39	0.73	0.87
Ansic-05	15.3013	37.6063	0	22.2	38.4	37.46	24.95	18.63	4.67	23.84	4.63	1.56	8.25	1.38	10.00	2.75	8.47	1.14	7.82	1.11	13.61	0.40	0.75	0.86
			25	19.8	38.3	37.96	25.23	18.40	4.70	24.09	4.75	1.52	8.29	1.40	10.14	2.61	8.54	1.18	8.02	1.13	14.53	0.39	0.72	0.89
			50	17.5	38.3	38.50	25.70	19.13	5.17	24.53	4.83	1.48	8.40	1.43	10.33	2.89	8.75	1.21	8.20	1.13	13.34	0.39	0.69	0.86
			89	15.6	38.5	38.50	25.81	20.16	4.86	24.60	5.46	1.52	8.48	1.44	10.27	2.67	8.81	1.22	8.16	1.16	14.40	0.41	0.67	0.89
Ansic-06	15.3041	37.7380	0	22.1	38.4	34.68	23.22	17.49	4.58	21.92	4.77	1.36	7.65	1.30	9.40	2.41	7.91	1.09	7.34	1.02	14.37	0.39	0.68	0.90
			25	17.5	38.4	37.07	25.01	17.77	4.71	24.17	4.64	1.46	8.28	1.40	10.07	2.66	8.45	1.18	7.83	1.12	13.93	0.38	0.70	0.88
			50	16.6	38.4	37.23	25.12	17.98	4.88	23.71	5.28	1.48	8.10	1.41	10.16	2.67	8.69	1.18	7.86	1.12	13.96	0.37	0.68	0.90
			92	15.4	38.5	39.53	26.54	20.13	4.99	25.31	5.38	1.57	8.73	1.47	10.66	2.83	8.94	1.26	8.21	1.20	13.99	0.40	0.69	0.88

Y/Ho ratios, Ce and Eu anomalies and t_3 index calculated for tetrad effect in the Gd–Tb–Dy–Ho group are also listed. Measurement uncertainties as in Table 1. Long., longitude; Lat., latitude; Temp., temperature; Sal., salinity.

yses carried out on SOL-1 were also used to verify the potential contribution of trace elements released from the chemicals used during concentration procedures. Details of the adopted technical procedures are fully described in Censi et al. (2007).

2.3. Suspended particulate matter (SPM)

SPM (about 0.015 g) was collected on a 0.2-μm Millipore filter from approximately 6 l of seawater. In order to collect both its labile and detrital fractions, the samples of seawater were not acidified before filtration (FengFu et al., 1997). After weighing, with ±0.01 mg accuracy, the recovered fractions were digested as reported in Censi et al. (2004) using a microwave oven (CEM Mars 5) equipped with TFM vessels to which an acid solution was added with proportions $HCl/HNO_3/HF = 4:4:4$ (total volume = 12 ml). After complete dissolution, the acid excess was removed to incipient dryness using a Microvap™ apparatus. Then, 5 ml of nitric acid (65% v/v) were added to the sample solutions, diluted to 100 ml with Millipore® water, and finally transferred into clean 100 ml polycarbonate bottles. The solutions were analysed directly after dilution (1:50) with 5% HNO_3 (Merck, ULTRAPURE®) and addition of a Rh internal standard (0.97 nmol l^{-1}).

2.4. Volcanic ash

Mineralogical composition of the ash samples was investigated by X-ray diffractometry, using a Ni-filtered Cu-Kα radiation and a Siemens 5500 X-ray spectrometer.

The 10–50 μm fraction of freshly erupted volcanic ash selected for kinetic experiments was ultrasonically cleaned in pure water (18.2 MΩ cm^{-1}) for 12 h, and then dried. The specific surface area of ash was estimated at 0.44 $m^2 g^{-1}$, and the ash surface to water volume during the cleaning procedure ranged between 5435 and 1089 cm^{-1}, as a function of the solid particle size (10–50 μm). Although this procedure may potentially cause unpredictable dissolution of the finest particles, it turned out to be appropriate for removing any soluble substances adhering to the particle surfaces, thus avoiding formation of secondary materials and consequent deposition on activated surfaces of larger particles. Four different 50 g aliquots of this fraction were placed in 500 ml Nalgene® bottles. The final ash surface to volume ratio of the solution used during leaching experiments (S/V) was fixed between 110 and 22 cm^{-1}. These S/V values are comparable to those used by Möller and Giese (1997) and Techer et al. (2001) during leaching experiments of powder basaltic materials in pure water under closed system conditions. Moreover, Etna's eruptive activity of 2001 was the most intense recorded in the last 300 years, with an estimated quantity of $\sim 7 \times 10^6$ m^3 of volcanic ejecta (Behncke and Neri, 2003; Clocchiatti et al., 2004; Lautze et al., 2004). Assuming that the accumulation of volcanic ash (size <50 μm) deposited at the sea surface of the sampled area (approximately ~800 km^2) for the entire period of Etna's eruption is comparable to that measured at the roof of the Department of Geology of Catania (~2.15 cm m^{-2}/5 days), we estimated a S/V ratio ranging between 52 and 5 cm^{-1}, from 1 m and 10 m deep water layers, respectively. This is of the same order of magnitude as that used during the kinetic experiments. However, we do not know the dispersal effects caused by local winds on the main ash plume, or potential influences on the settling dynamics of particles through the water column. This information should be taken into account when comparing the results of kinetic experiments with those obtained from natural systems.

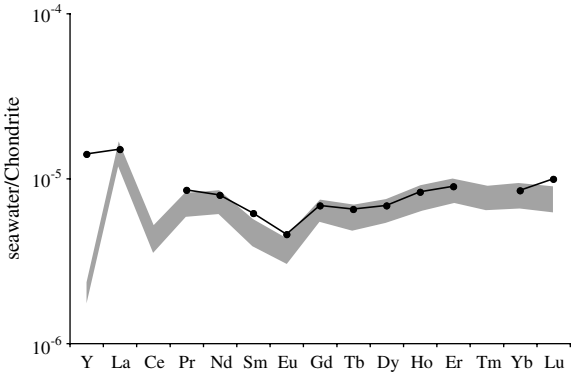

Fig. 2. Chondrite-normalised YREE patterns of the analysed seawater (grey band). Chondrite-normalised YREE patterns of Levantine Intermediate Water (•) are reported from Bau et al. (1997). YREE abundances in chondrite are derived from Sun and McDonough (1989).

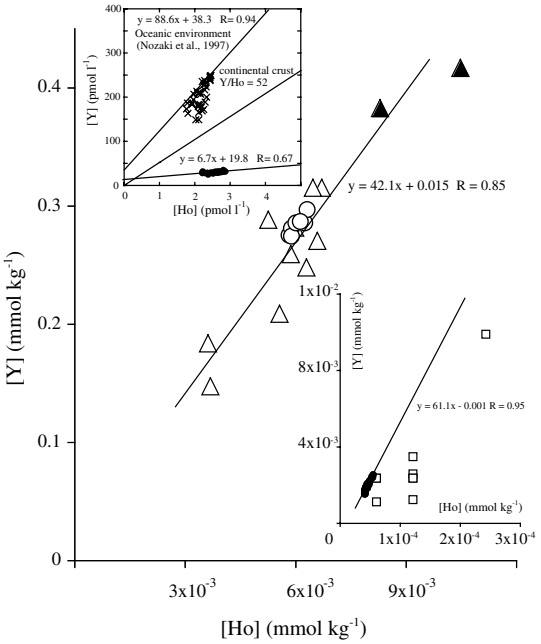

Fig. 3. Yttrium and holmium contents in seawater samples and SPM. Concentration values for plagioclase, clinopyroxene, amphibole phenocrysts, and 2001 lavas are reported from Viccaro et al. (2006). The ranges of Y and Ho contents measured in Central Mediterranean seawater during the oceanographic cruise BANSIC 2000 (Censi et al., 2007) and the linear trend of Nozaki et al. (1997), calculated for the open ocean, are reported for comparison.

Table 3
Sampling depth and YREE concentrations measured in the SPM at the six sampling stations

	Depth (m)	Y (μmol kg^{-1})	La (μmol kg^{-1})	Ce (μmol kg^{-1})	Pr (μmol kg^{-1})	Nd (μmol kg^{-1})	Sm (μmol kg^{-1})	Eu (μmol kg^{-1})	Gd (μmol kg^{-1})	Tb (μmol kg^{-1})	Dy (μmol kg^{-1})	Ho (nmol kg^{-1})	Er (nmol kg^{-1})	Tm (nmol kg^{-1})	Yb (nmol kg^{-1})	Lu (nmol kg^{-1})	Y/Ho	Ce/Ce*	Eu/Eu*	t_3
Ansic-01	0	2.09	4.55	6.51	0.95	3.44	0.45	0.11	0.36	59.19	307.73	45.00	131.85	17.59	86.07	15.78	46.44	0.73	0.77	1.17
	25	1.80	4.32	6.45	0.89	3.23	0.44	0.10	0.35	54.69	290.85	41.42	121.91	17.45	83.41	15.31	43.43	0.77	0.76	1.15
	50	1.54	4.30	6.44	0.89	3.19	0.44	0.10	0.35	54.01	287.11	40.68	120.32	17.41	82.50	15.22	37.93	0.77	0.75	1.16
	87	1.71	4.37	6.49	0.93	3.45	0.45	0.10	0.39	56.13	311.48	42.01	127.60	17.80	84.62	15.49	40.82	0.76	0.74	1.15
Ansic-02	0	2.43	4.62	7.14	1.01	3.62	0.47	0.14	0.38	69.24	356.44	52.56	149.09	20.83	98.29	17.15	46.16	0.78	0.95	1.22
	25	1.92	4.47	6.94	0.93	3.37	0.45	0.11	0.36	56.57	299.28	43.17	128.04	18.05	93.26	15.90	44.52	0.79	0.81	1.15
	50	1.71	4.38	6.83	0.92	3.33	0.44	0.10	0.36	55.83	294.19	41.90	123.95	17.64	91.05	15.49	40.81	0.80	0.76	1.16
	96	1.87	4.42	6.88	0.93	3.47	0.45	0.11	0.37	57.27	296.78	44.27	124.80	17.84	89.85	15.68	42.25	0.79	0.76	1.13
Ansic-03	0	2.55	4.95	7.24	1.01	3.70	0.49	0.14	0.40	71.34	357.25	55.01	155.02	23.47	97.78	18.25	46.39	0.75	0.92	1.20
	25	1.98	4.54	7.03	0.94	3.45	0.48	0.11	0.37	57.55	312.44	43.82	132.58	18.33	97.49	16.23	45.14	0.79	0.76	1.16
	50	1.79	4.32	6.77	0.90	3.17	0.44	0.10	0.35	53.08	269.24	41.72	123.21	17.46	91.75	15.29	42.85	0.80	0.76	1.09
	91	1.90	4.33	6.93	0.91	3.29	0.44	0.10	0.35	57.31	306.71	42.45	125.42	17.55	86.92	15.36	44.71	0.82	0.77	1.19
Ansic-04	0	2.41	4.87	7.05	0.99	3.66	0.49	0.13	0.38	68.60	371.83	54.04	142.00	22.37	97.21	17.61	44.52	0.75	0.85	1.22
	25	1.97	4.48	6.67	0.93	3.48	0.45	0.11	0.37	56.78	301.38	45.02	133.75	18.17	93.16	16.09	43.78	0.76	0.78	1.13
	50	1.91	4.33	6.57	0.88	3.22	0.43	0.09	0.35	54.67	297.29	43.84	122.17	17.48	90.00	15.33	43.49	0.78	0.72	1.14
	84	1.85	4.35	6.59	0.91	3.37	0.45	0.10	0.36	55.39	296.58	45.28	124.52	17.64	87.46	15.55	40.83	0.77	0.76	1.11
Ansic-05	0	2.24	4.89	7.05	0.97	3.50	0.47	0.12	0.38	64.72	351.09	49.15	136.95	19.58	92.07	16.99	45.68	0.75	0.87	1.22
	25	1.98	4.47	6.66	0.93	3.31	0.45	0.11	0.36	56.49	318.50	46.59	127.56	18.10	91.14	15.89	42.50	0.76	0.76	1.14
	50	1.55	4.24	6.51	0.87	3.16	0.43	0.10	0.35	51.44	300.07	41.59	123.82	17.13	90.39	15.03	37.27	0.79	0.75	1.14
	89	1.69	4.31	6.54	0.90	3.20	0.44	0.10	0.35	58.10	299.15	41.26	127.82	17.56	89.57	15.25	40.93	0.77	0.78	1.21
Ansic-06	0	2.19	4.81	6.97	0.95	3.47	0.47	0.10	0.36	62.77	331.91	49.04	139.56	18.28	91.89	16.19	44.69	0.75	0.75	1.20
	25	2.05	4.45	6.47	0.92	3.30	0.45	0.11	0.36	56.09	313.96	48.07	136.86	17.67	92.40	15.82	42.68	0.74	0.79	1.12
	50	1.67	4.26	6.47	0.90	3.08	0.41	0.10	0.35	53.77	279.92	41.11	120.25	17.21	89.98	15.14	40.58	0.77	0.79	1.13
	92	1.70	4.32	6.67	0.92	3.21	0.44	0.11	0.36	54.32	286.93	41.57	123.67	17.49	91.37	15.45	41.00	0.79	0.79	1.12

Y/Ho ratios, Ce and Eu anomalies and t_3 index calculated for tetrad effect in the Gd–Tb–Dy–Ho group are also listed. Measurement uncertainties as in Table 1.

The trace-element-free seawater (described in Section 2.2) was used to fill each bottle with the aliquots of volcanic ash (500 ml per bottle).

Results from leaching experiments are generally reported for pure water (e.g., Möller and Giese, 1997; Bach and Irber, 1998; Bau et al., 1998), and adsorption processes are investigated in a solution of known composition (Coppin et al., 2002; Takahashi et al., 2004). In order to compare the results obtained from our leaching experiment with literature data, we favoured the use of a trace-element-free seawater. However, we appreciate that the presence of the complexes of trace elements in "true" seawater significantly influences the interaction of the ligands with labile trace elements present in the volcanic ash. Actually, it could effectively render the trace-element-free seawater similar to an "activated" solution, with ligands that are more available for binding with new trace elements, thus influencing the extent of REE enrichment as well as any fractionation between individual REE (e.g., Y and Ho) during water–rock interactions. Thus, directly extrapolating the results of the kinetic experiments to the behaviour of YREEs in the sampled Mediterranean seawater should be considered with great caution.

The pH of the solution in each bottle was adjusted to 6.0 at the beginning of the experiments and then allowed to drift freely. After 15 days, the measured pH reached values of ~7, in good agreement with evidence reported by Crovisier et al. (2003). During suspension experiments of basalts in pure water, they observed an increase of initial pH values from 5.5 to 7.5 after 14 days at temperatures ranging from 3 to 60 °C.

Each bottle was sealed and placed in a thermostatic bath at 25 °C. This temperature value was chosen because it is similar to that measured in the surface waters at the sampling stations (Table 2). One bottle was removed from the bath after 15, 30, 90 and 180 days, respectively, and the ash was separated by filtration.

The full-length of the kinetic experiment was approximately defined according to an average particle (mean diameter <50 μm) settling speed calculated by Schmidt et al. (2002) for coastal and open areas of the Mediterranean basin. The authors estimated a particle's average residence time in surface waters of about 50 days, and a following average settling speed of ~1–5 m day^{-1} through the water column.

All samples were analysed with a high resolution HR-ICP-MS (ThermoFinniganMAT Element 2) using 0.97 nmol l^{-1} Rh as internal standard at the Laboratory of Geochemistry of the Department of Geology (University of Catania). This includes the eluted fractions representative of seawater from the Ionian sea and those from the kinetic experiments, as well as all the digested solutions representative of both suspended particulate matter and volcanic ash involved in the kinetic experiments.

The exponential best fit equations used to analyse the results of the leaching experiments for all the YREEs, Y/Ho ratios, and Ce anomalies were calculated using a simple least squares minimisation method (KaleidaGraph 3.6®).

3. RESULTS

3.1. Dissolved phase

The dissolved YREE concentrations at the six sampling stations, the geographical locations, and the measured temperature and salinity are listed in Table 2.

Fig. 1 shows that dissolved YREEs are more abundant in seawater from the southern sampling stations located closer to the centre of volcanic plume. Moreover, YREE contents progressively increase with depth in all the studied stations. YREE contents range from about 150 nmol l^{-1} in the shallowest waters and continuously increase up to ~170 nmol l^{-1} in the deepest water layer (~90 m). Chondrite-normalised YREE patterns (Fig. 2) for the seawater

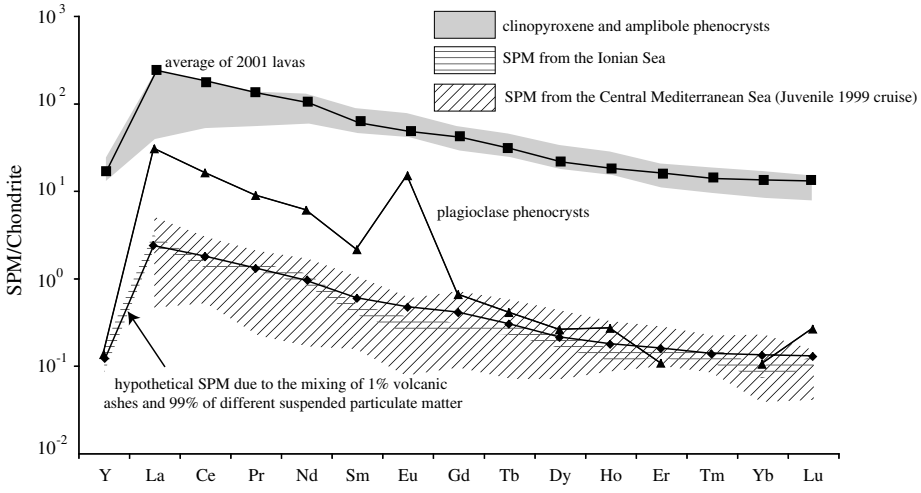

Fig. 4. Chondrite-normalised YREE patterns of suspended particulate matter in samples of seawater from different sampling stations. The chondrite-normalised patterns of other materials are reported for comparison. YREE abundances in chondrite are derived from Sun and McDonough (1989).

Table 4
YREE concentrations measured in the leaching solutions and ash during the kinetic experiment at the end of each interaction time

	15 days	1 month	3 months	6 months
Dissolved fraction				
Y	521.5	752.5	1143.6	1275.4
La	2920.0	5960.0	9910.0	12270.0
Ce	3069.2	5366.7	11461.8	15772.5
Pr	376.2	538.9	1040.2	1309.7
Nd	1254.0	1643.4	2641.5	3063.7
Sm	177.17	247.31	358.04	446.63
Eu	33.40	87.42	169.93	276.27
Gd	72.42	126.06	172.15	278.54
Tb	14.61	16.56	23.38	36.53
Dy	49.3	72.8	105.2	123.3
Ho	14.98	18.01	22.80	25.16
Er	30.03	46.77	71.79	95.86
Tm	3.12	6.71	10.79	11.27
Yb	23.18	45.26	57.02	62.89
Lu	0.99	1.73	8.41	9.90
Y/Ho	52.15	47.03	45.74	42.51
Ce/Ce*	0.83	0.78	0.75	0.74
Eu/Eu*	0.76	1.34	1.84	2.21
Ash				
Y	343.5	341.1	337.2	335.9
La	742.58	712.18	672.68	649.08
Ce	1115.07	1083.51	1037.71	1012.64
Pr	116.88	112.77	104.89	99.64
Nd	409.35	403.30	393.93	379.78
Sm	85.00	81.09	76.35	67.04
Eu	22.24	20.27	16.98	13.51
Gd	57.30	55.76	50.89	49.25
Tb	7.11	6.81	6.25	6.13
Dy	36.25	34.15	30.97	30.09
Ho	6.18	5.92	5.59	5.45
Er	15.90	14.83	12.89	11.94
Tm	1.98	1.93	1.79	1.76
Yb	14.51	14.04	13.04	11.87
Lu	1.91	1.75	1.67	1.58
Y/Ho	55.5	57.6	60.3	61.6
Ce/Ce*	0.83	0.84	0.84	0.83
Eu/Eu*	1.01	1.01	0.98	0.94
Log (K_d)				
Y	2.8	2.7	2.5	2.4
La	2.4	2.1	1.8	1.7
Ce	2.6	2.3	2.0	1.8
Pr	2.5	2.3	2.0	1.9
Nd	2.6	2.4	2.2	2.1
Sm	2.7	2.5	2.4	2.3
Eu	2.9	2.6	2.1	1.9
Gd	2.9	2.6	2.4	2.3
Tb	2.9	2.7	2.4	2.3
Dy	2.9	2.7	2.4	2.3
Ho	2.8	2.6	2.4	2.3
Er	2.7	2.5	2.3	2.2
Tm	2.7	2.5	2.3	2.2
Yb	2.7	2.6	2.4	2.3
Lu	2.7	2.5	2.3	2.2
EAF				
Y	1.5	2.2	3.4	3.8
La	3.9	8.4	14.7	18.9
Ce	2.8	4.9	10.7	14.9
Pr	3.2	4.7	9.4	12.1
Nd	2.4	3.8	6.7	7.8
Sm	2.0	2.8	4.1	5.2
Eu	1.2	2.8	7.1	12.3
Gd	1.2	2.3	4.0	5.2
Tb	1.2	2.0	3.6	4.8
Dy	1.3	2.2	3.6	4.7
Ho	1.5	2.4	3.8	4.6
Er	2.0	3.0	4.7	5.8
Tm	1.9	3.1	4.6	6.2
Yb	1.8	2.7	4.1	5.6
Lu	2.1	3.2	4.9	6.4

Measurement uncertainties as in Table 1. Apparent distribution coefficients (K_d), pH values measured at the different steps of the kinetic experiments and easily accessible fraction (EAF) calculated for YREEs are also given. YREE concentrations are given in micromoles per litre (Ash) as nanomoles per litre (dissolved fraction).

samples are very similar to those reported for the Levantine Intermediate Waters (LIW) by Bau et al. (1997). However, their absolute Y contents are about one order of magnitude lower, ranging from 33 to 42 pmol l^{-1} (Table 2), compared to a mean value of ~250 pmol l^{-1} measured in seawater from the Eastern Mediterranean Basin. An average Y/Ho molar ratio of 14.7 ± 0.9 was measured in the collected samples, with a linear regression for the dissolved Y and Ho contents showing a slope $d[Y]/d[Ho] = 6.7$. This value is lower than that of 88.6 calculated by Nozaki et al. (1997) in open oceanic environments (Fig. 3).

3.2. Suspended particulate matter

The YREE concentrations of SPM are reported in Table 3. The chondrite-normalised YREE distribution of SPM (Fig. 4) falls inside the range of analogous samples collected during the "Juvenile 1999" cruise (Censi et al., 2004) in the Sicily Channel. Moreover, the chondrite-normalised YREE patterns in SPM samples evidence the same LREE/HREE fractionation observed in lavas and enclosed clinopyroxene and hastingsite phenocrysts erupted during the volcanic activity of Mount Etna during 2001 (Viccaro et al., 2006). The YREE distribution in SPM collected in the Ionian sea appears significantly weighted by leaching effects on ash present in seawater (Fig. 4). This is suggested by the chondrite-normalised YREE pattern of a mixture of ~1% fraction of pristine volcanic products and a ~99% fraction of different suspended materials (basically consisting of sedimentary lithogenic products, organic debris, and authigenic materials).

The linear regression of Y/Ho ratios calculated for the SPM samples yields a slope of ~61, with an average Y/Ho ratio close to 43. These values are consistent with the linear regression line calculated for lavas, pyroxene, and amphibole phenocrysts erupted by Etna during 2001 (Fig. 3). It is much more difficult to compare SPM samples with plagioclase phenocrysts erupted during the same eruptive activity of 2001, which do not show any systematic trend of Y/Ho ratios.

3.3. Kinetic experiments

For the YREE contents of both the leaching solutions and leached volcanic ash, the apparent distribution coefficients (K_d) were calculated according to the expression:

$$K_d = \frac{[\mathrm{YREE}]_{ash}}{[\mathrm{YREE}]_{sol}}. \quad (1)$$

The "easy accessible fraction" (EAF) represents the concentration ratio of a given element both in leachate and leaching solution. These were calculated according Bau et al. (1998) for the investigated trace elements, and are given in Table 4.

The YREE release from newly-formed volcanic ash under the experimental conditions discussed in Section 2.4 is well-described by a first order kinetic model. This process distinctly leads to the release of YREEs in the liquid phase. The concentration of each element in the solution during the consecutive time steps can be fitted by the expression:

$$[\mathrm{YREE}_i]_{SW} = m_1 + m_2\{1 - \exp(-m_3 t)\}, \quad (2)$$

where $[\mathrm{YREE}_i]_{SW}$ represents the concentration value of each Rare Earth Element and Yttrium in the leaching solution. The values for kinetic constants m_i are given in Table 5. The time evolution of YREE concentrations in the dissolved phase during the kinetic experiments is shown in Fig. 5 and reported in Table 4.

During the experiments, the dissolved Y/Ho ratios progressively decrease to a final value of ~43. The Ce anomaly in the dissolved phase also changes during the kinetic experiments according to the expression:

$$\left[\frac{Ce}{Ce^*}\right]_{SW} = 0.74 + 0.20\{\exp(-0.66t)\}, \quad (3)$$

where the Ce anomaly is defined following Alibo and Nozaki (1999) by:

$$\frac{Ce}{Ce^*} = \frac{2[Ce]_n}{[La]_n + [Pr]_n}, \quad (4)$$

where subscript n indicates the normalised concentration value of each element, and Ce^* is the average between the La and Pr normalised concentrations. The ratio slightly decreases to a value of 0.74 after 6 months, as shown in Fig. 5.

4. DISCUSSION

4.1. Kinetic experiments

The effects of YREE release in seawater during the leaching experiments, well-fitted by Eq. (2) for Y and Ho, respectively, suggest a faster release of holmium than of yttrium (Fig. 5). This evidence cannot be exclusively explained in terms of coherent mineral weathering because both Y and Ho, due to their similar ionic radii, undergo the same fate during the crystallisation processes of primary minerals (Shannon, 1976; Bau, 1996). Therefore, the observed Y/Ho variations are better explained through the formation of alteration minerals, which in turn, induce different scavenging effects on these elements. At the same time, the development of the negative Ce anomaly, usually observed in seawater (Elderfield and Greaves, 1982), also appears to be enhanced by the scavenging due to the affinity of Ce^{IV} for particles. Therefore, the observed Y/Ho–Ce/Ce^* covariance (Fig. 6) constitutes a geochemical signature which shows the effects of the YREE release during ash dissolution, and the differential fractionation of these elements by sorption onto newly-formed alteration products. Seawater samples from the surface layers of the Ionian sea show Y/Ho and Ce/Ce^* values (Fig. 6) that closely approximate the linear trend calculated for the same ion ratios measured in dissolved phase during the kinetic experiments ($Ce/Ce^* = 0.25Y/Ho + 0.01$; $r = 0.97$). This suggests that the YREE partitioning between dissolved and suspended

Table 5
Kinetic constants, and relative standard deviations, of the exponential fitting curves

	m_1	$\pm\sigma$	m_2	$\pm\sigma$	m_3	$\pm\sigma$	LS (1 h) (nmol l^{-1})	Ionian SW (pmol l^{-1})
Y	0.223	0.036	1.07	0.03	0.25	0.02	61.26	236.27
La	0.120	1.529	12.40	1.25	0.22	0.08	6.18	29.31
Ce	0.467	0.143	16.23	0.18	0.14	0.01	129.88	11.06
Pr	0.143	0.038	1.30	0.04	0.15	0.02	29.20	3.61
Nd	0.275	0.041	2.86	0.03	0.23	0.01	79.27	20.24
Sm	0.128	0.029	0.36	0.04	0.14	0.05	12.59	3.59
Eu	0.000	0.015	0.39	0.07	0.08	0.03	2.70	0.97
Gd	0.018	0.025	0.28	0.02	0.18	0.06	18.27	4.16
Tb	0.004	0.002	0.04	0.00	0.13	0.03	3.59	0.80
Dy	0.027	0.011	0.16	0.01	0.14	0.05	1.94	8.49
Ho	0.004	0.002	0.03	0.00	0.21	0.05	0.89	2.45
Er	0.016	0.005	0.07	0.00	0.18	0.04	3.34	5.44
Tm	0.002	0.001	0.01	0.00	0.12	0.08	0.02	1.28
Yb	0.018	0.006	0.07	0.02	0.10	0.06	0.10	8.93
Lu	0.001	0.001	0.01	0.00	0.18	0.06	0.01	1.41

YREE concentrations measured in leaching solution (LS) after 1 h of interaction between ash and seawater. YREE concentrations in Ionian seawaters measured during the Juvenile 1999 Cruise (Censi et al., 2004) are given for comparison. Measurement uncertainties for leaching solution and Ionian seawater as in Table 1. Elemental concentrations are given in micromoles per litre.

phases in natural seawater may be influenced by the dissolution of volcanic material, mainly in the surface waters. However, this process occurs in seawater under open system conditions, whereas kinetic experiments strictly document effects in a closed system. These differences may justify the observed discrepancies between the trends calculated for the experimentally and naturally investigated systems.

The K_d values show a progressive increase from Ce to Sm and medium REEs. After 15 days of leaching, a negative Eu anomaly occurs, possibly due to release of this element in dissolved phase after longer leaching periods

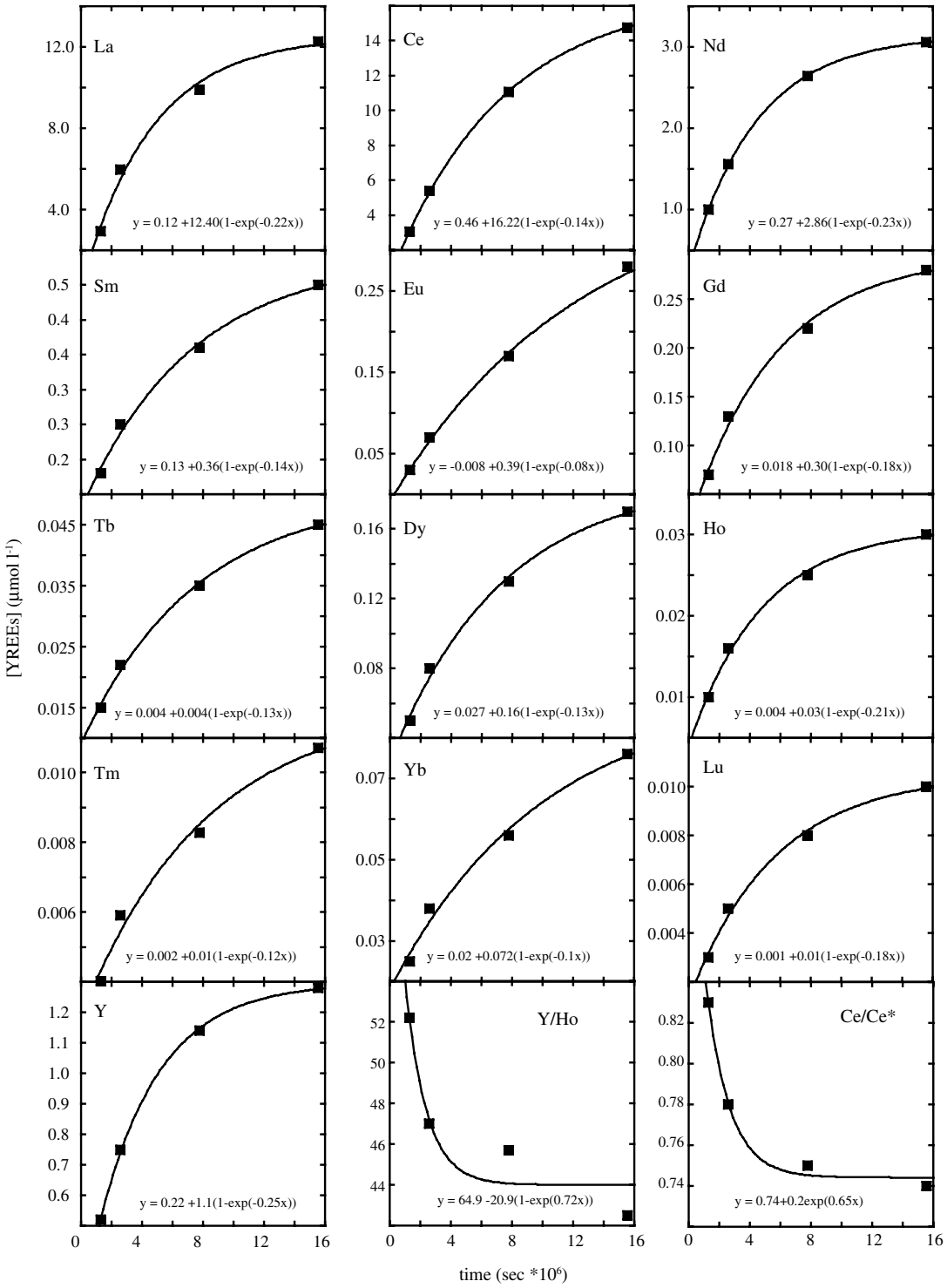

Fig. 5. Variation of YREE concentrations, Y/Ho ratios, and Ce anomalies in dissolved phase during kinetic experiments.

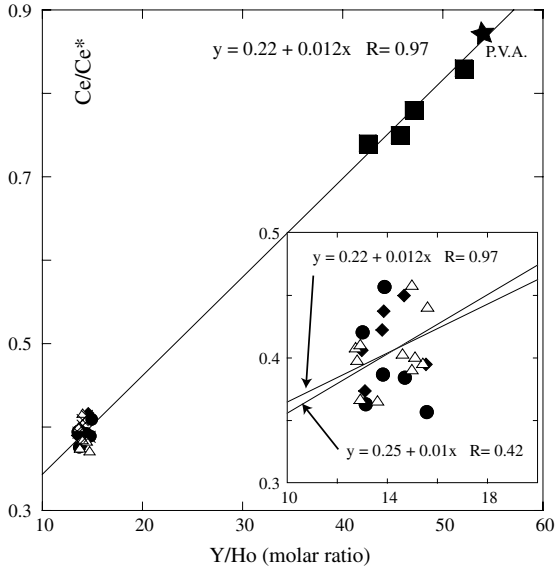

Fig. 6. Ce/Ce* versus Y/Ho during leaching experiments. The regression line was calculated among the values of composition measured in pristine volcanic ash (P.V.A.), and those obtained after progressive leaching of P.V.A. at 15, 30, 90 and 180 days (■). Ce/Ce* versus Y/Ho values from surface (△), 50 m depth (♦), and bottom seawater (●) analysed in this work are also reported.

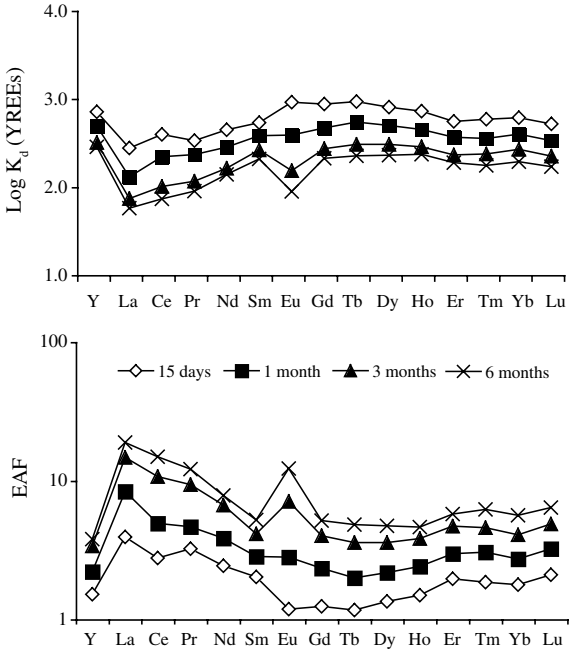

Fig. 7. Apparent distribution coefficients (K_d) and easily accessible fraction (EAF) calculated for YREEs at different times during kinetic experiments.

(Fig. 7). Actually, europium is only partially released during the first leaching period, being preferentially incorporated in the highly-resistant plagioclase phenocrysts. This particular Eu behaviour is highlighted by the variation of the Eu anomaly, defined similarly to the Ce anomaly (Eq. (4)), as:

$$\frac{Eu}{Eu^*} = \frac{2[Eu]_n}{[Sm]_n + [Gd]_n}, \quad (5)$$

which ranges from 0.8 (after 15 days) to 2.2 (after 6 months).

The effects of ash alteration in the experiment solution are well illustrated in Fig. 8, where elemental maps and related BSE (back-scattered electron) images depict an evident alteration rim on the surface of a volcanic grain after 1 month of interaction with the leaching solution. The alteration rim, mainly derived from a glassy precursor, is enriched in Na, Al, K, and Ca, whereas other Mg-Fe rich mineral phases appear corrosion free. This evidence agrees with the high rate of YREE removal at the beginning of the leaching experiments because they are enclosed in poorly crystalline materials. Furthermore, the effects of ash mineralogy on the mobility of YREEs are also suggested by chondrite-normalised patterns calculated in the dissolved phase during the leaching experiments (Fig. 9).

The change of pH values during the kinetic experiments (Fig. 10) reflects the effects of rapid glass dissolution and slow precipitation of newly-formed cryptocrystalline montmorillonite-type products, as suggested by Crovisier et al. (1987, 2003). The alteration of ash particles by rapid hydration of a pristine glassy fraction may lead to the formation of poorly crystallised (palagonitic) products, whose further "hydration" may be responsible for the observed pH increase during the experiment. Moreover, Oelkers and Gislason (2001) and Oelkers (2001), showed that dissolution of volcanic glass is related to a proton-metal ion exchange on glass surfaces which directly produces a pH increase in the leaching solution.

The tendency of lanthanides to remain mainly in dissolved form is also corroborated by: (i) the lack of LREE fractionation with respect to HREE, (ii) the absence of a minimum of dissolved Pr content (Byrne and Kim, 1993; Byrne et al., 1996; Liu et al., 1997), and (iii) the preferential Yttrium scavenging on solid matter.

4.2. Dissolved phase

Y/Ho values (mole ratio) in chondritic materials cluster around 52 (Sun and McDonough, 1989). During primary processes, such as magma formation and related crystallisation of igneous minerals, Y shows strong geochemical similarities with HREEs from Gd to Lu (mainly Ho), due to their highly similar charges and ionic radii in solids (Shannon, 1976). The chemical processes that do not cause fractionation of Y with respect to Ho and HREEs are defined as "CHARAC (CHarge And RAdius Controlled) processes" by Bau (1996). Conversely, if Y and Ho are involved in non-CHARAC processes, such as during aqueous reactions in which the electronic configuration of the elements plays an important role, the above mentioned Y–Ho similarities diminish because Y^{3+} and Ho^{3+} have different electronic external configurations, $[Kr]4d^0$ and $[Xe]4f^{10}$, respectively.

These non-CHARAC processes influence the YREE concentration in such a way that their normalised patterns

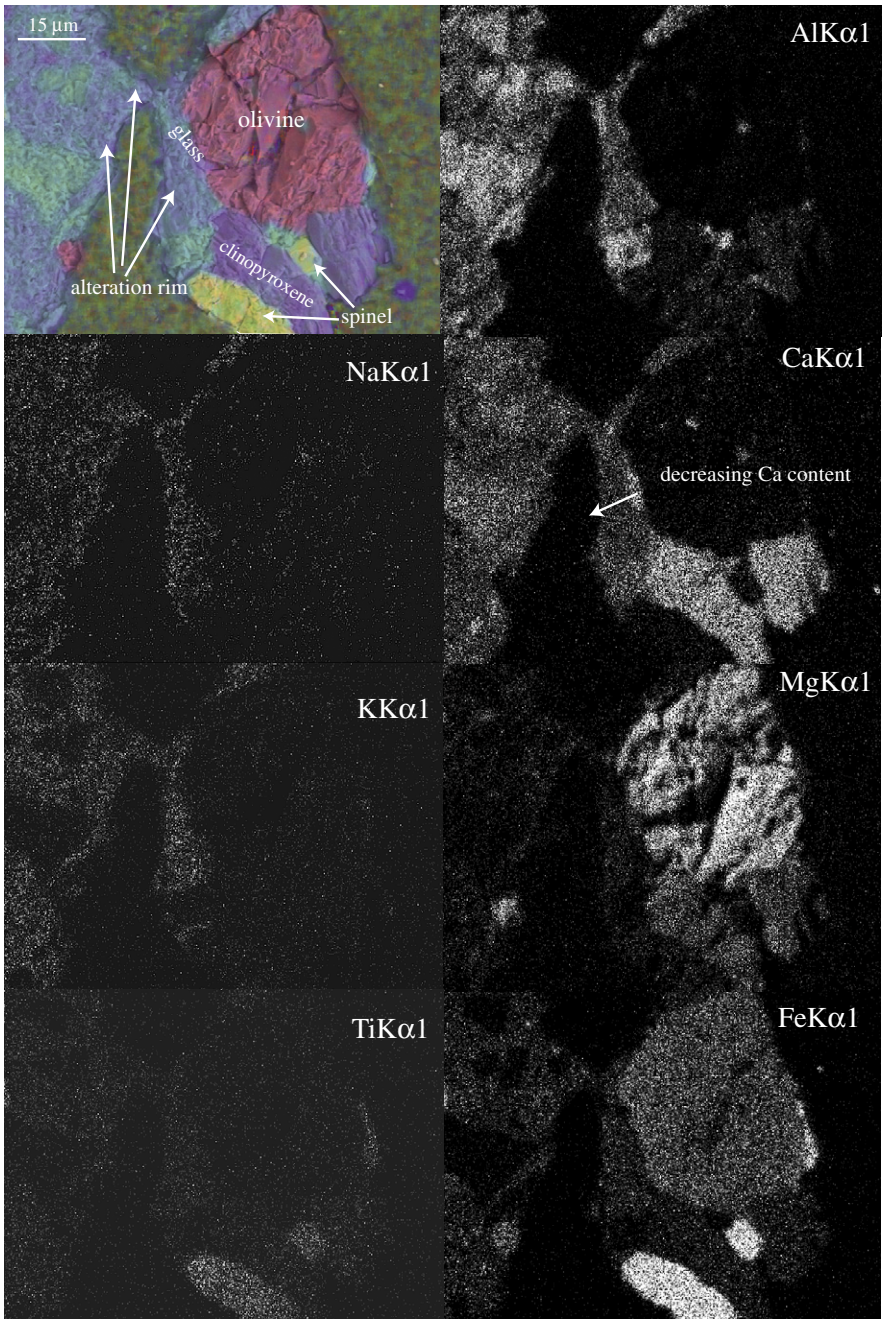

Fig. 8. BSE image and related elemental maps of volcanic ash (enclosed in resin) used during kinetic experiments after 1 month of interaction. The different minerals are labelled and glass rim and alteration products are evidenced.

can be subdivided into four "segments" (La–Nd, Pm–Gd, Gd–Ho, Er–Lu), called tetrads (Masuda and Ikeuchi, 1979). This behaviour is called the "tetrad effect" and is usually associated with adsorption, co-precipitation, dissolution, complexation, and/or ligand-exchange reactions. A detailed description of the tetrad effect and its theoretical interpretation is presented by Masuda and Ikeuchi (1979).

Upward concave, W-shaped tetrad effects are observed during solid–liquid heterogeneous reactions when the character of the lanthanide/ion–ligand bond is weakly covalent. Upward convex, M-shaped tetrad effects are interpreted as the result of increasing covalency of the REE–O bond onto the solid surface and a lowering of Racah parameters with respect to the aquo-complex system (Hotta and Ueda, 2003). On the other hand, shape and amplitude of the tetrad effect occurring in the YREE path depicted during solid–liquid reactions can be quantified by the equation:

$$t_i = \sqrt{\frac{[\mathrm{REE}]_2 \times [\mathrm{REE}]_3}{[\mathrm{REE}]_1 \times [\mathrm{REE}]_4}}, \quad (6)$$

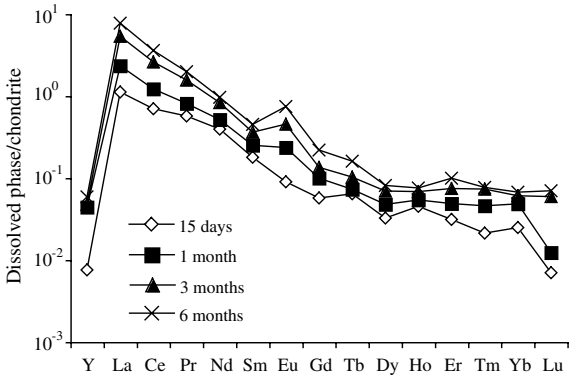

Fig. 9. Chondrite-normalised YREE patterns calculated at the end of each period of interaction between ash and seawater. YREE abundances in chondrite are derived from Sun and McDonough (1989).

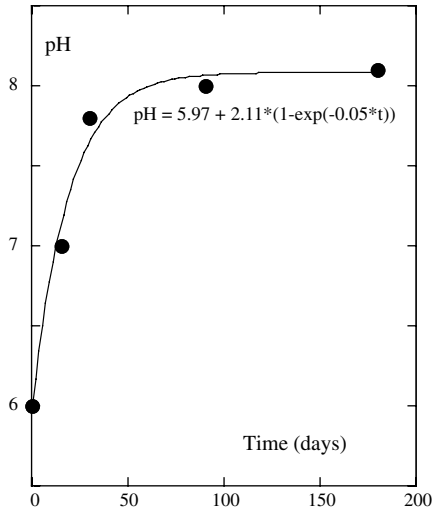

Fig. 10. Evolution of pH values during ash–seawater exchange experiment.

(Irber, 1999). They are also influenced by competition between solution and dissolved complexation processes (Kim et al., 1991; Quinn et al., 2006). In Eq. (6), t_i is the extent of the tetrad effect, and $[REE]_{1-4}$ are the normalised REE concentrations of the first, second, third, and fourth elements of a given tetrad. Values of t_i higher or lower than one identify a convex and concave tetrad effect, respectively.

Similarly, Y^{3+} and Ho^{3+} also show different behaviour because of differences in the covalent character. Y/Ho ratios can increase above the classic value of 52 (Nozaki et al., 1997; Censi et al., 2007) due to interactions with oxygen present in the silicate minerals and aqueous ligands in seawater, and during surface complexation in heterogeneous equilibria (Bau, 1999; Quinn et al., 2004).

The products of the Etna eruption during summer 2001 systematically show consistent averages of Y/Ho ratio. These vary from 47 ± 0.7 (for measured lavas) to 44.5 ± 5 for both clinopyroxene and amphibole phenocrysts, with the exception of plagioclase which exhibits large variations of the Y/Ho ratio from 19.5 to 40.8 (Viccaro et al., 2006). The range of values of Y/Ho is in agreement with the range of variability of the CHARAC ratios for basalts (Y/Ho = 44.5–70.5; Bau, 1996). Therefore, the anomalously low Y/Ho values measured in seawater cannot directly result from ash release, but may be subsequently induced by processes causing Yttrium removal from the dissolved pool in surface waters. In particular, the effects of co-precipitation and adsorption can be assumed to be responsible for the fractionation of YREEs at the particulate-seawater interface (Balistrieri et al., 1981; De Carlo and Koeppenkastrop, 1991; Koeppenkastrop and De Carlo, 1992, 1993). This is particularly evident during Mn–Fe oxyhydroxides formation, which induces a progressive increase of Y/Ho ratios in the dissolved phase to values higher than 52, due to preferential Ho scavenging effects (Bau et al., 1998; Bau, 1999; Ohta and Kawabe, 2001). Evidence from alteration effects on the ash leached during the kinetic experiments suggest differential YREE sorption processes onto montmorillonite-type mineral surfaces that could explain the preferential removal of Y. This mechanism may be due to the preferential formation under alkaline pH conditions of Yttrium and OH^- inner-sphere complexes onto particle edges of montmorillonite (Takahashi et al., 2004).

The narrow range of variability evidenced by the Y/Ho ratios along the water column (Fig. 1) emphasises a rapid alteration of the glassy fraction present in the volcanic ash (even in the first metre of the water column). However, the results of Crovisier et al. (2003) suggest that such a rapid alteration induces an increase of specific surface area of suspended ash. These are well-reflected in the studied samples by the increase of YREE contents along the water columns.

The occurrence of alteration products on the surfaces of basaltic materials was previously well-documented and associated with the formation of nontronite and Fe-saponite (Techer et al., 2001). In our samples, scanning electron microscopy (SEM) and X-ray analyses of SPM show evident effects of corrosion on the volcanic ash collected in surface water layers (Fig. 11). The alteration products of ash are clearly enriched in Al, Na, and K, suggesting a replacement of the original glassy fractions by smectitic minerals. This was suggested by Crovisier et al. (2003) and here is hypothesised from the leaching experiments. Firstly, Humphris (1984) suggested that the mobility of YREEs during weathering processes of volcanic material is mainly influenced by: (i) temperature, (ii) aptitude of newly-formed minerals to accommodate YREEs, and (iii) chemistry of the interacting fluids. Therefore, because YREE release during weathering of volcanic materials is related to lanthanide distribution coefficients during the primary crystallisation phase of existing volcanic minerals (Shibata et al., 2006), it follows that the occurrence of poorly crystalline matter in ash represents a source of Lanthanides during weathering (Bach and Irber, 1998; Bau et al., 1998).

In the studied ash samples, YREEs are potentially enriched in the glassy fraction and/or on the surface of the alteration minerals because they cannot be accommodated

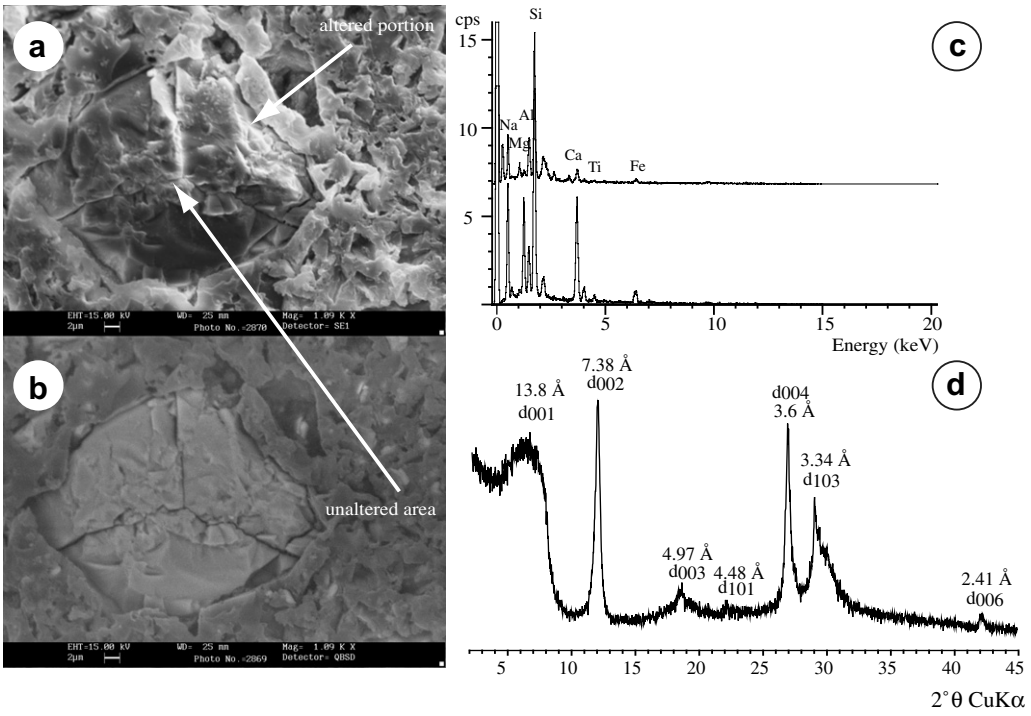

Fig. 11. Secondary electrons image of volcanic ash materials (enclosed in resin) in SPM (from surface sample collected at Ansic-04). (a) Topography by secondary electrons image; (b) back-scattered electrons image. (c) EDS spectra of volcanic material, both in pristine and altered areas, which evidence Na and Fe leaching in the weathered part of grains. (d) XRD spectrum of volcanic ash collected in water samples.

into the lattice of the primary minerals (Rollinson, 1993). Consequently, they are more easily accessible to leaching (Humphris, 1984). Moreover, the studied ash samples appear free from accessory minerals (such as phosphates), which are generally enriched in YREEs, while they are rich in clinopyroxene, Ca-rich plagioclase, olivine, and Ti–Fe spinel.

Montmorillonite-type alteration products appear as adequate substrates to produce YREE fractionation in seawater. Lanthanide adsorption onto montmorillonite-type alteration products can be separated into two different modalities that depend on adsorption mechanisms: cationic exchange in interlayer position and surface complexation from silanol and aluminol groups at the edge of particles (Tertre et al., 2005). The first process is strongly influenced by ionic strength and does not depend on pH (Coppin et al., 2002; Tertre et al., 2005). On the contrary, pH conditions strongly influence surface complexation that occurs with an inner-sphere mechanism (Takahashi et al., 2004; Tertre et al., 2005). The chondrite-normalised patterns of YREEs in our seawater samples also suggest an important contribution to the YREE fractionation effects from the alteration of volcanic SPM (Fig. 12). In particular:

- The recorded La enrichment in seawater can be related to preferential release of light REEs from volcanic ash, as suggested by the leaching experiments and by similar results reported by Bau et al. (1998). These authors explain this phenomenon with the occurrence of higher concentrations of LREEs in more easily alterable glassy and interstitial materials of basaltic rocks;
- The observed negative Eu anomalies can be related to the characteristic Eu distribution in the plagioclase crystal structure (McKay, 1989). Because plagioclase is one of the most chemically resistant minerals (Stefansson, 2001), the Eu anomalies may suggest an incomplete dissolution of volcanic products in seawater;
- The absence of evident tetrad effects (ranging $0.8 \leqslant t_3 \leqslant 1.0$) for the Gd–Ho tetrad suggests that dissolved REEs exist as strong dissolved complexes in the studied water masses. Under these conditions they are involved in adsorption processes on SPM surfaces as outer sphere organic complexes (Takahashi et al., 1999; Davranche et al., 2004, 2005), or are subjected to competition between carbonate complexation and surface complexation on surface of suspended particles (Quinn et al., 2006).

4.3. Suspended particulate matter (SPM)

Chondrite-normalised YREE patterns calculated for SPM confirm the general picture that emerges from the analysis of the dissolved fraction with regard to the origin of these elements and their fate during weathering of volcanic ash in seawater. These patterns record the dissolution of pyroclastic materials coming from Mount Etna through the

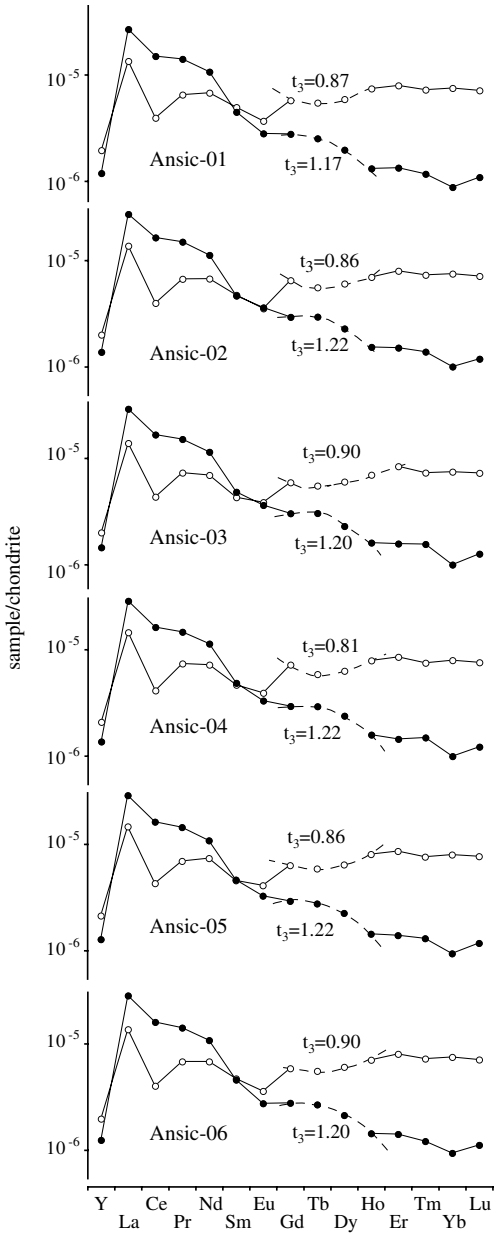

Fig. 12. Chondrite-normalised YREE patterns calculated for SPM (full circles) and seawater (open circles) samples collected from the surface layer. Chondrite-normalised YREEs in SPM are divided by 10^6. YREE abundances in chondrite are derived from Sun and McDonough (1989). The t_3 value for the tetrad effect in the Gd-Ho range is reported.

occurrence of tetrad effects in Gd–Ho interval. The t_3 amplitude in SPM collected from surface waters falls between $1.17 \leqslant t_3 \leqslant 1.22$, and is higher than that occurring in the co-existing seawater. Evidence of early REE release by selective dissolution of fresh ash components is progressively overprinted by a more complete dissolution of pyroxene, olivine, and finally plagioclase, as particles sink along the water column. The progressive dissolution of volcanic ash is accompanied by a decrease in the tetrad effect in SPM that ranges from 1.20 to 1.25 in surface waters, to about 1.05–1.00 in deeper layers. This suggests a direct relationship between the tetrad effect and the S/V ratio, which decreases along the water column. Also, the classic effect reported by Monecke et al. (2002) of coupled M-shaped and W-shaped tetrad effects recorded in SPM and seawater, respectively (Fig. 12), implies a strong relationship between weathering of volcanic ash and YREE enrichment in seawater.

5. CONCLUSIONS

Input of lithogenic material is one of the most important sources of Lanthanides (Yttrium and REEs) in Mediterranean seawater. This study demonstrates that the delivery of large amounts of pyroclastic products from the explosive activity of Mount Etna during the last few years may have modified the distribution of these trace elements in the seawater of the investigated area (Ionian Sea). Dissolution of ash and formation of alteration minerals in SPM both seem to alter the distribution of YREEs in seawater. The availability of both altered pyroclastic material and large amounts of newly formed clay materials in SPM causes large LREEs/HREEs fractionation.

The anomalously low Y/Ho ratios recorded in seawater are explained in terms of Y transfer to surfaces of alteration products. Significant M-type tetrad effects are observed only in chondrite normalised SPM patterns, suggesting that this material represents a source of REEs to the seawater. Limited scavenging of REEs takes place on the surfaces of weathered volcanic mineral particles by generation of weak outer-sphere surface complexes unable to produce significant W-type tetrad effects in the Gd–Ho range in the dissolved phase. Finally, Yttrium that, in alkaline conditions, forms OH-inner-sphere complexes on particle edges of montmorillonite-type structures, decouples with respect to Ho and allows the dissolved phase to assume anomalously low Y/Ho ratios.

ACKNOWLEDGMENTS

This work was financially supported by a grant from the University of Catania (Funds 60%, responsible P. Censi). We are indebted to S. Speziale for his suggestions and critical reviews on a preliminary version of the manuscript. Many thanks are given to P. Sclafani for her careful job of English revision. Moreover, the authors are very grateful to E.H. De Carlo, two anonymous reviewers, and R. Byrne (AE) for their careful and dedicated job of critical revision of a first and second version of the manuscript.

REFERENCES

Alibo D. S. and Nozaki Y. (1999) Rare earth elements in seawater: particle association, shale-normalization, and Ce oxidation. *Geochim. Cosmochim. Acta* **63**, 363–372.

Aubert D., Stille P., Probst A., Gauthier-Lafaye F., Pourcelot L. and Del Nero M. (2002) Characterization and migration of atmospheric REE in soils and surface waters. *Geochim. Cosmochim. Acta* **66**, 3339–3350.

Bach W. and Irber W. (1998) Rare earth element mobility in the oceanic lower sheeted dyke complex: evidence from geochemical data and leaching experiments. *Chem. Geol.* **151**, 309–326.

Balistrieri L. S., Brewer P. G. and Murray J. W. (1981) Scavenging residence times of trace metals and surface chemistry of sinking particles in the deep ocean. *Deep-Sea Res.* **28A**, 101–121.

Bau M. (1996) Controls on the fractionation of isovalent trace elements in magmatic and aqueous systems: evidence from Y/Ho, Zr/Hf, and lanthanide tetrad effect. *Contrib. Miner. Petrol.* **123**, 323–333.

Bau M. (1999) Scavenging of dissolved yttrium and rare earths by precipitating iron oxydroxide: experimental evidence for Ce oxidation, Y/Ho fractionation, and lanthanide tetrad effect. *Geochim. Cosmichim. Acta* **63**, 67–77.

Bau M. and Dulski P. (1996) Anthropogenic origin of positive gadolinium anomalies in river waters. *Earth Planet. Sci. Lett.* **143**, 245–255.

Bau M., Möller P. and Dulski P. (1997) Yttrium and lanthanides in eastern mediterranean seawater and their fractionation during redox cycling. *Mar Chem.* **56**, 123–131.

Bau M., Usui A., Pracejus B., Mita N., Kanai Y., Irber W. and Dulski P. (1998) Geochemistry of low-temperature water–rock interaction: evidence from natural waters, andesite, and iron-oxyhydroxide precipitates at Nishiki-numa iron-spring, Hokkaido, Japan. *Chem. Geol.* **151**, 293–307.

Bau M., Alexander B., Chesley J. T., Dulski P. and Brantley S. L. (2004) Mineral dissolution in the Cape Cod aquifer, Massachusetts, USA: I. Reaction stoichiometry and impact of accessory feldspar and glauconite on strontium isotopes, solute concentrations, and YREEs distribution. *Geochim. Cosmochim. Acta* **68**, 1199–1216.

Behncke B. and Neri M. (2003) The July–August 2001 eruption of Mt. Etna (Sicily). *Bull. Volcanol.* **65**, 461–476.

Butler R. A., Covington A. K. and Whitfield M. (1985) The determination of pH in estuarine waters. II: Practical considerations. *Oceanol. Acta* **8**, 433–439.

Byrne R. H. and Kim K. H. (1993) Rare earth precipitation and coprecipitation behavior: the limiting role of PO_4^{3-} on dissolved rare earth concentrations in seawater. *Geochim. Cosmochim. Acta* **57**, 519–526.

Byrne R. H. and Li B. Q. (1995) Comparative complexation behavior of the rare-earths. *Geochim. Cosmochim. Acta* **59**, 4575–4589.

Byrne R. H. and Liu X. W. (1998) A coupled riverine–marine fractionation model for dissolved rare earths and yttrium. *Aquat. Geochem.* **4**, 103–121.

Byrne R. H., Xuewu L. and Schijf J. (1996) The influence of phosphate coprecipitation on rare earth distributions in natural waters. *Geochim. Cosmochim. Acta* **60**, 3341–3346.

Cantrell K. J. and Byrne R. H. (1987) Rare earth element complexation by carbonate and oxalate ions. *Geochim. Cosmochim. Acta* **51**, 597–605.

Censi P., Mazzola S., Sprovieri M., Bonanno A., Patti B., Punturo R., Spoto S. E., Saiano F. and Alonzo G. (2004) Rare earth elements distribution in seawater and suspended particulate of the Central Mediterranean Sea. *Chem. Ecol.* **20**, 323–343.

Censi P., Spoto S. E., Nardone G., Saiano F., Punturo R., Di Geronimo S. E., Mazzola S., Bonanno P., Patti B., Sprovieri M. and Ottonello D. (2005) REE and yttrium distribution in mangrove coastal water systems. The western Gulf of Thailand. *Chem. Ecol.* **21**, 255–277.

Censi P., Larocca D., Saiano F., Placenti F. and Bonanno A. (2007) Recognition of water masses according to geochemical signatures in the Central Mediterranean sea: Y/Ho ratio and REE behaviour. *Chem. Ecol.* **23**, 139–155.

Clocchiatti R., Condomines M., Guenot N. and Tanguy J. C. (2004) Magma changes at Mount Etna: the 2001 and 2002–2003 eruptions. *Earth Planet. Sci. Lett.* **226**, 397–414.

Coppin F., Berger G., Bauer A., Castet S. and Loubet M. (2002) Sorption of lanthanides on smectite and kaolinite. *Chem. Geol.* **182**, 57–68.

Crovisier J. L., Honnorez J. and Eberhart J. P. (1987) Dissolution of basaltic glass in seawater: mechanism and rate. *Geochim. Cosmochim. Acta* **51**, 2977–2990.

Crovisier J.-L., Advocat T. and Dussossoy J.-L. (2003) Nature and role of natural alteration gels formed on the surface of ancient volcanic glasses (natural analogs of waste containment glasses). *J. Nucl. Mater.* **321**, 91–109.

Davranche M., Pourret O., Gruau G. and Dia A. (2004) Impact of humate complexation on the adsorption of REE onto Fe oxyhydroxide. *J. Colloid Interf. Sci.* **277**, 271–279.

Davranche M., Pourret O., Gruau G., Dia A. and Le Coz-Bouhnik M. (2005) Adsorption of REE(III)–humate complexes onto MnO_2: experimental evidence for cerium anomaly and lanthanide tetrad effect suppression. *Geochim. Cosmochim. Acta* **69**, 4825–4835.

De Carlo E. H. and Koeppenkastrop D. (1991) Sampling and methods of characterization of surface reactivity. In *Marine Particles: Analysis and Characterization, Geophysical Monograph* (eds. D. C. Hurd and D. W. Spencer), vol. 63, pp. 419–427.

Demianov P., De Stefano C., Gianguzza A. and Sammartano S. (1995) Equilibrium studies in natural waters: speciation of phenolic compounds in synthetic seawater at different salinities. *Environ. Toxicol. Chem.* **14**, 767–773.

Dickson A. G. (1993a) pH buffers for sea water media based on the total hydrogen ion concentration scale. *Deep-Sea Res.* **40**, 107–118.

Dickson A. G. (1993b) The measurement of sea water pH. *Mar. Chem.* **44**, 131–142.

Elderfield H. (1988) the oceanic chemistry of rare-earth elements. *Philos. Trans. R. Soc. London* **325**, 105–126.

Elderfield H. and Greaves M. J. (1982) The rare earth elements in seawater. *Nature* **296**, 214–219.

Elderfield H., Upstill-Goddard R. and Sholkovitz E. R. (1990) The rare earth elements in rivers, estuaries, and coastal seas and their significance to the composition of ocean waters. *Geochim. Cosmochim. Acta* **54**, 971–991.

FengFu F., Shinotsuka K., Ebihara M. and Akagi T. (1997) Distribution ratio of dissolved and particulate REE in surface coastal waters. *Geochem. J.* **31**, 303–314.

Goldberg E. D., Koide M., Schmitt R. A. and Smith R. H. (1963) Rare-earth distributions in the marine environment. *J. Geophys. Res.* **68**, 4209–4217.

Goldstein S. J. and Jacobsen S. B. (1988) Rare earth elements in river waters. *Earth Planet. Sci. Lett.* **89**, 35–47.

Greaves M. J., Rudnicki M. and Elderfield H. (1991) Rare earth elements in the Mediterranean Sea and mixing in the Mediterranean outflow. *Earth Planet. Sci. Lett.* **103**, 169–181.

Hannigan R. E. and Sholkovitz E. R. (2001) The development of middle rare earth element enrichments in freshwaters: weathering of phosphate minerals. *Chem. Geol.* **175**, 495–508.

Hotta T. and Ueda K. (2003) Construction of microscopic model for f-electron systems on the basis of *j–j* coupling scheme. *Phys. Rev.* **B67**, 104518.1–104518.16.

Humphris S. (1984) The mobility of the rare earth elements in the crust. In *Rare Earth Element Geochemistry*. Elsevier, Amsterdam, pp. 317–342.

Irber W. (1999) The lanthanide tetrad effect and its correlation with K/Rb, Eu/Eu*, Sr/Eu,Y/Ho and Zr/Hf of evolving peraluminous granite suites. *Geochim. Cosmochim. Acta* **63**, 489–508.

Kim K. H., Byrne R. H. and Lee J. L. (1991) Gadolinium behavior in seawater: a molecular basis for gadolinium anomalies. *Mar. Chem.* **36**, 107–120.

Klungness G. D. and Byrne R. H. (2000) Comparative hydrolysis behavior of the rare earths and yttrium: influence of temperature and ionic strength. *Polyedron* **19**, 99–107.

Koeppenkastrop D. and De Carlo E. H. (1992) Sorption of rare-earth elements from seawater onto synthetic mineral particles: an experimental approach. *Chem. Geol.* **95**, 251–263.

Koeppenkastrop D. and de Carlo E. H. (1993) Uptake of rare earth elements from solution by metal oxides. *Environ. Sci. Technol.* **27**, 1796–1802.

Koeppenkastrop D., De Carlo E. H. and Roth M. (1991) A method to investigate the interaction of rare earth elements with metal oxides in aqueous solution. *J. Radioanal. Nucl. Chem.* **151**, 337–346.

Lautze N. C., Harris A. J. L., Bailey J. E., Ripepe M., Calvari S., Dehn J., Rowland S. K. and Jones K. E. (2004) Pulsed lava effusion at Mount Etna during 2001. *J. Volcanol. Geotherm. Res.* **137**, 231–246.

Lee J. H. and Byrne R. H. (1992) Examination of comparative rare earth element complexation behavior using linear free-energy relationships. *Geochim. Cosmochim. Acta* **56**, 1127–1137.

Liu X., Byrne R. H. and Schijf J. (1997) Comparative coprecipitation of phosphate and arsenate with Yttrium and the Rare Earths: the influence of solution complexation. *J. Solution Chem.* **26**, 1187–1198.

Luo Y.-R. and Byrne R. H. (2004) Carbonate complexation of yttrium and the rare earth elements in natural waters. *Geochim. Cosmochim. Acta* **68**, 691–769.

Masuda A. and Ikeuchi Y. (1979) Lanthanide tetrad effect observed in marine environment. *Geochem. J.* **13**, 19–22.

McKay G. A. (1989) Partitioning of Rare Earth Elements between major silicate minerals and basaltic melts. In *Geochemistry and Mineralogy of Rare Earth Elements, Reviews in Mineralogy* (eds. B. R. Lipin and G. A. McKay), vol. 21, pp. 45–77.

Millero F. J. (1992) Stability constants for the formation of rare earth inorganic complexes as a function of ionic strength. *Geochim. Cosmochim. Acta* **56**, 3123–3132.

Millero F. J., Zhang J.-Z., Fiol S., Sotolongo S., Roy R. N., Lee K. and Mane S. (1993) The use of buffers to measure the pH of sea water. *Mar. Chem.* **44**, 143–152.

Möller P. and Giese U. (1997) Determination of easily accessible metal fractions in rocks by batch leaching with acid cation-exchange resin. *Chem. Geol.* **137**, 41–55.

Möller P., Dulski P. and Luck J. (1992) Determination of rare earth elements in seawater by inductively coupled plasma-mass spectrometry. *Spectrochim. Acta* **47B**, 1379.

Monecke T., Kempe U., Monecke J., Sala M. and Wolf D. (2002) Tetrad effect in rare earth element distribution patterns: a method of quantification with application to rock and mineral samples from granite-related rare metal deposits. *Geochim. Cosmochim. Acta* **66**, 1185–1196.

Nozaki Y., Zhang J. and Amakawa H. (1997) The fractionation between Y and Ho in the marine environment. *Earth Planet. Sci. Lett.* **148**, 329–340.

Oelkers E. H. (2001) A general kinetic description of multi-oxide silicate mineral and glass dissolution. *Geochim. Cosmochim. Acta* **65**, 3703–3719.

Oelkers E. H. and Gislason S. R. (2001) The mechanism, rates, and consequences of basaltic glass dissolution: I. An experimental study of the dissolution rates of basaltic glass as a function of aqueous Al, Si, and oxalic acid concentration at 25 °C and pH = 3 and 11. *Geochim. Cosmochim. Acta* **65**, 3671–3681.

Ohta A. and Kawabe I. (2001) REE(III) adsorption onto Mn dioxide (δ-MnO_2) and Fe oxyhydroxides: Ce(III) oxidation by δ-MnO_2. *Geochim. Cosmochim. Acta* **65**, 695–703.

Paulson A. J. (1986) The effects of flow rate and pre-treatment on the analyses of trace metals in estuarine and coastal seawater by Chelex-100. *Anal. Chem.* **58**, 183–187.

Pichler T., Ian Ridley W. and Nelson E. (1999) Low-temperature alteration of dredged volcanics from the southern Chile ridge: additional information about early stages of seafloor weathering. *Mar. Geol.* **159**, 155–177.

Pourret O., Davranche M., Gruau G. and Dia A. (2007) Competition between humic acid and carbonates for rare earth elements complexation. *J. Colloid Interf. Sci.* **305**, 25–31.

Quinn K. A., Byrne R. H. and Schijf J. (2004) Comparative scavenging of Yttrium and the Rare Earth Elements in seawater: competitive influences of solution and surface chemistry. *Aquat. Geochem.* **10**, 59–80.

Quinn K. A., Byrne R. H. and Schijf J. (2006) Sorption of yttrium and rare earth elements by amorphous ferric hydroxide: influence of solution complexation with carbonate. *Geochim. Cosmochim. Acta* **70**, 4151–4165.

Rollinson H. (1993) *Using Geochemical Data: Evaluation, Presentation, Interpretation*. Longman, Harlow, UK.

Schmidt S., Andersen V., Belviso S. and Marty J. C. (2002) Strong seasonality in particle dynamics of north-western Mediterranean surface waters as revealed by $^{234}Th/^{238}U$. *Deep-Sea Res. I* **49**, 1507–1518.

Shannon R. D. (1976) Revised effective ionic radii and systematic studies of interatomic distances in halides and chalcogenides. *Acta Cryst.* **B25**, 925–946.

Shibata S. N., Tanaka T. and Yamamoto K. (2006) Crystal structure control of the dissolution of rare earth element in water–mineral interactions. *Geochem. J.* **40**, 437–446.

Sholkovitz E. R. (1993) The geochemistry of rare earth elements in the Amazon River estuary. *Geochim. Cosmochim. Acta* **57**, 2181–2190.

Sholkovitz E. R., Elderfield H., Smymczak R. and Casey K. (1999) Island weathering: river sources of rare earth elements to the Western Pacific Ocean. *Mar. Chem.* **68**, 39–57.

Sonke J. E. and Salters V. J. M. (2006) Lanthanide–humic substances complexation. I. Experimental evidence for a lanthanide contraction effect. *Geochim. Cosmochim. Acta* **70**, 1495–1506.

Stefansson A. (2001) Dissolution of primary minerals of basalt in natural waters: I. Calculation of mineral solubilities from 0 °C to 350 °C. *Chem. Geol.* **172**, 225–250.

Sun S. S. and McDonough W. F. (1989) Chemical and isotopic systematics of oceanic basalts. In *Magmatism in the Ocean Basins. Geol. Soc. Am. Bull.* (eds. D. Saunders and M. J. Norry), vol. 42, pp. 313–345.

Tachikawa K., Jeandel C., Vangriesheim A. and Dupré B. (1999) Distribution of rare earth elements and neodymium isotopes in suspended particles of the tropical Atlantic Ocean (EUMELI site). *Deep-Sea Res.* **46**, 733–755.

Takahashi Y., Kimura T., Kato Y. and Minai Y. (1999) Speciation of europium(III) sorbed on a montmorillonite surface in the presence of polycarboxylic acid by laser-induced fluorescence spectroscopy. *Environ. Sci. Technol.* **33**, 4016–4021.

Takahashi Y., Yoshida H., Sato N., Hama K., Yusa Y. and Shimizu H. (2002) W- and M-type tetrad effects in REE patterns for water–rock systems in the Tono uranium deposit, central Japan. *Chem. Geol.* **184**, 311–335.

Takahashi Y., Tada A. and Shimizu H. (2004) Distribution patterns of Rare Earth ions between water and Montmorillonite and its relation to the sorbed species of the ions. *Anal. Sci.* **20**, 1301–1306.

Techer I., Advocat T., Lancelot J. and Liotard J-M. (2001) Dissolution kinetics of basaltic glasses: control by solution

chemistry and protective effect of the alteration film. *Chem. Geol.* **176**, 235–263.

Tertre E., Berger G., Castet S., Loubet M. and Giffaut E. (2005) Experimental sorption of Ni^{2+}, Cs^{+} and Ln^{3+} onto a montmorillonite up to 150 °C. *Geochim. Cosmochim. Acta* **69**, 4937–4948.

Tertre E., Berger G., Simoni E., Castet S., Giffaut E., Loubet M. and Catalette H. (2005) Europium retention onto clay minerals from 25 to 150 °C: experimental measurements, spectroscopic features and sorption modelling. *Geochim. Cosmochim. Acta* **70**, 4563–4578.

Tombácz E. and Szekeres M. (2004) Colloidal behavior of aqueous montmorillonite suspensions: the specific role of pH in the presence of indifferent electrolytes. *Appl. Clay Sci.* **27**, 75–94.

Viccaro M., Ferlito C., Cortesogno L., Cristofolini R. and Gaggero L. (2006) Magma mixing during the 2001 event at Mount Etna (Italy): effects on the eruptive dynamics. *J. Volcanol. Geotherm. Res.* **149**, 139–159.

Associate editor: Robert H. Byrne